Rats spontaneously perceive global motion direction of drifting plaids

Giulio Matteucci[1,2,*], Benedetta Zattera[1,3,*], Rosilari Bellacosa Marotti[1], and Davide Zoccolan[1,#]

1. Visual Neuroscience Lab, International School for Advanced Studies (SISSA), Trieste, 34136, Italy

2. Current address: Department of Basic Neurosciences, University of Geneva, Geneva, 1206, Switzerland

3. Current address: Friedrich Miescher Institute for Biomedical Research (FMI), Basel, 4058, Switzerland

**These authors contributed equally to this work*

Corresponding author

Davide Zoccolan

International School for Advanced Studies (SISSA)

Via Bonomea, 265 34136 Trieste (TS) ITALY

Office: +39 040 3787 701 Fax: +39 040 3787 702

E-mail: zoccolan@sissa.it

Abstract

Computing global motion direction of extended visual objects is a hallmark of primate high-level vision. Although neurons selective for global motion have also been found in mouse visual cortex, it remains unknown whether rodents can combine multiple motion signals into global, integrated percepts. To address this question, we trained two groups of rats to discriminate either gratings (G group) or plaids (i.e., superpositions of gratings with different orientations; P group) drifting horizontally along opposite directions. After the animals learned the task, we applied a visual priming paradigm, where presentation of the target stimulus was preceded by the brief presentation of either a grating or a plaid. The extent to which rat responses to the targets were biased by such prime stimuli provided a measure of the spontaneous, perceived similarity between primes and targets. We found that gratings and plaids, when uses as primes, were equally effective at biasing the perception of plaid direction for the rats of the P group. Conversely, for G group, only the gratings acted as effective prime stimuli, while the plaids failed to alter the perception of grating direction. To interpret these observations, we simulated a decision neuron reading out the representations of gratings and plaids, as conveyed by populations of either component or pattern cells (i.e., local or global motion detectors). We concluded that the findings for the P group are highly consistent with the existence of a population of pattern cells, playing a functional role similar to that demonstrated in primates. We also explored different scenarios that could explain the failure of the plaid stimuli to elicit a sizable priming magnitude for the G group. These simulations yielded testable predictions about the properties of motion representations in rodent visual cortex at the single-cell and circuitry level, thus paving the way to future neurophysiology experiments.

Introduction

Extracting global motion direction of visual objects is crucial to guide behavior in many ethological contexts (1,2). Such computation has been widely studied in the dorsal stream of primates, and, in particular, in the middle temporal area (MT) of the macaque (3). This area is known to receive direct input from neurons in primary visual cortex (V1), which signal the "local" direction of moving elements (e.g., edges) in their small, localized, receptive fields (RF). MT units appear to combine the afferent V1 inputs in such a way to acquire selectivity for the "global" motion direction of visual objects (or patterns) made of multiple local edges (4). The leading hypothesis emerging from the primate literature is that this is achieved by integrating the local motion signals carried by V1 afferents over different spatial positions, directions and frequencies (3–5). Such integration is necessary, because the local output of any V1-like edge detector is intrinsically ambiguous insofar global motion is concerned. Any local output can be generated by infinite combinations of global object directions and speeds. This ambiguity is at the core of what is known, in the psychophysics literature, as the "aperture problem" (6–8): only by combining information from multiple, local, moving-edge detectors, it is possible to infer global motion direction. Achieving a circuit level understanding of such computation remains a key question in visual neuroscience.

Over the past 10 years, the development of a wide array of tools for the dissection of neural circuits (9–13), combined with the demonstration of advanced visual behaviors in mice and rats (14,15), has fostered the use of rodents as model systems to study visual cortical processing. This led some investigators to look for the signature of motion integration in the rodent brain (16–18). Inspired by monkey studies (19–22), they recorded the responses of mouse visual cortical neurons to drifting gratings and coherent plaids − i.e., complex visual patterns made of two overlapping gratings with the same contrast and speed, but

moving along independent directions. These stimuli have been widely used to investigate motion integration in human and non-human primates since they enable to clearly distinguish local- from global-based motion responses. A plaid, in fact, has two well-defined local motion components and a global direction that is different from the local ones, while, for a grating, the local and global directions coincide (5). By employing these stimuli, mouse visual neurons were classified as "pattern" (i.e., responsive to global motion) or "component" (i.e., responsive to local motion). The majority of neurons amenable to such classification fell into the component category, but a small fraction of pattern units was reported in V1 (17,18) and in two extrastriate areas, the lateromedial (LM) and rostrolateral (RL) areas (16). However, the relevance of such tiny population of pattern cells in determining mouse motion perception was left untested [but see further discussion of (17) below].

Even if a few studies tested the ability of rats and mice to discriminate the dominant motion direction of random dot kinematograms (23–26) (RDKs: a task linked to motion integration, since it requires spatial pooling of local motion cues), no study ever probed the ability of rodents to integrate into a global motion percept multiple oriented elements moving along different directions. In addition, all the studies employing RDKs explicitly trained the animals in the direction discrimination task. Critically, this prevented assessing the spontaneous, purely perceptual motion integration abilities of naïve rodents. In fact, if feedback (e.g., reward) is provided to an animal about the outcome of his perceptual choices, it may learn to associate a given stimulus to a given response category without necessarily perceiving the sensory quality that the investigator intends to associate to that category (15,27,28). It would thus be impossible to infer from such kind of experiments whether the choices of the animal are driven by a general-purpose representation of global motion direction at the level of visual cortex (as the one found in monkey MT), or by the ability to learn abstract representations of arbitrary stimulus categories in higher-order association

areas involved in perceptual decision making, such as posterior parietal cortex (PPC) (29–32).

Only in (17) this confound was avoided, by monitoring the direction of the optokinetic nystagmus (OKN) while presenting plaids to naïve mice. The resulting bimodal distribution of OKN movements tracking both the local-components and the overall global directions of the stimulus is suggestive of mouse ability to spontaneously perceive global motion. However, this conclusion is affected by the intrinsic limitation of OKN-based experiments to probe cortical processing. In fact, OKN is a reflexive phenomenon that is known to be largely controlled by subcortical structures (33–35), while motion perception in direction discrimination tasks has been shown to rely heavily on visual cortex (26,36,37). As a result, it remains unclear whether rodents spontaneously combine independent motion signals (as those found in plaids) into integrated percepts of global motion direction.

Our study was designed to address this question and provide a thorough psychophysical assessment of rat ability to spontaneously perceive the global direction of drifting plaids. To this aim, we relied on a visual priming paradigm (27,28) that allowed measuring the perceptual similarity between gratings and plaids with the same global direction, without explicitly training the animals to associate these stimuli to the same response category.

Results and discussion

A visual priming paradigm to probe spontaneous perception of global motion direction

In the first phase of the study (the *training phase*), a group of 11 male Long-Evans rats (referred to as the G group in what follows) was trained to discriminate leftward- from

rightward-drifting gratings (Fig 1A, left), using the high-throughput behavioral rig described in (15) and previously employed in several investigations of rat object recognition (27,38–41). Another group of 10 rats (referred to as the P group in what follows) was trained to discriminate leftward- from rightward-drifting plaids with a *cross-angle* of 120º – i.e. composite patterns made of the superposition of two gratings drifting along directions that were 120º apart (Fig 1B, left). Rats that maintained at least a criterion performance of 75% correct choices over a four consecutive day period were moved to the second phase of the study to be tested with the priming paradigm (all rats starting the training phase managed to reach such criterion).

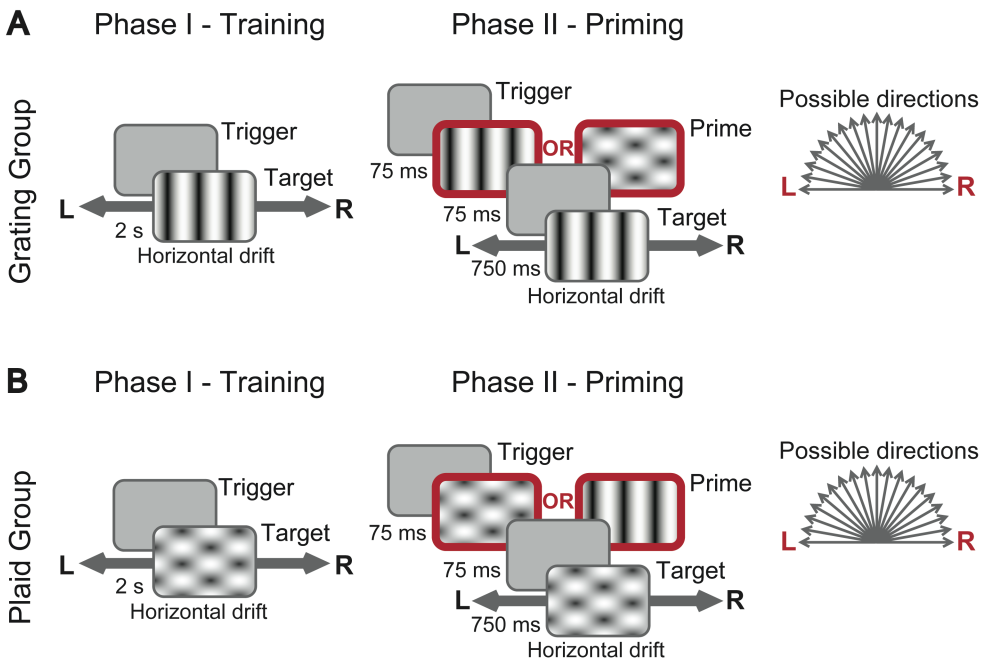

Fig 1 – Visual stimuli and discrimination tasks. (**A**) Discriminations tasks administered to the rats of the *grating* (G) *group*. During both the training (left) and priming (right) phases, a trial started when an animal triggered the central port of a 3-way licking sensor (see Materials and methods). During the training phase, a target grating (drifting either leftward or rightward) was presented immediately at the onset of each trial. To receive the reward, a rat had to lick the lateral port corresponding to the direction of motion of the presented target. During the priming phase, the structure of the task was similar, but at the onset of each trial, a drifting prime stimulus was presented for 75 ms, followed by a

75 ms blank screen and finally by the presentation of the target grating (lasting 750 ms). The prime stimulus could move in 19 possible directions (from 0° = right to 180° = left) and could be either a grating or a plaid. (**B**) Discriminations tasks administered to the rats of the *plaid* (P) *group*. The structure of the task was the same as in A, with the key difference that the target stimulus was a plaid instead of a grating (again drifting either leftward or rightward). In this case, the reward was delivered when a rat licked the lateral port corresponding to the global motion direction of the plaid.

In the priming paradigm, the "target" stimulus remained the same as in the training phase (i.e., G and P rats still had to report the direction of drifting gratings and plaids, respectively), but now the presentation of the target was preceded by the brief presentation (75 ms) of either a grating or a plaid drifting along one of 19 possible directions (from 0° = rightward to 180° = leftward, in steps of 10°; Fig 1 A-B, right). The identity (i.e., either grating or plaid) and the motion direction of such "prime" stimulus was randomly selected in each trial. In what follows, we refer to trials in which the identities of prime and target coincide as *identity-priming* condition (e.g., a grating prime stimulus followed by a grating target stimulus), whereas we refer to the opposite case as *cross-priming* condition (e.g., a plaid prime stimulus followed by a grating target stimulus). Critically, the rats kept receiving feedback (i.e., either reward or a time-out period in case of correct and incorrect choices, respectively) only about the correctness of their responses to the target stimuli. The identity and direction of the prime stimuli were never paired to either the leftward or rightward response categories. As such, the extent to which the prime stimuli were able to affect the choices of the rats was purely due to the spontaneous, perceived similarity between primes and targets. Assessing such similarity was the ultimate goal of our experiments, since it allowed understanding whether, in the cross-priming condition, the perceived motion direction of the plaids was the global one. Based on previous motion adaptation studies in humans (42) and on former priming/masking experiments carried out in rats (27,43–45), we

158 choose the duration of the prime and of the inter-stimulus interval (ISI) between prime and
159 target (75 ms each) in the attempt of inducing a strong priming effect – i.e., in the attempt of
160 biasing rats' responses to the target towards the motion direction of the prime.

161 In what follows, we will report the accuracy of rats at discriminating the motion
162 direction of a target stimulus as a function of its angular distance from the direction of the
163 prime stimulus that preceded it. As such, the resulting *priming curve* will range between two
164 extremes: 1) the case in which the direction of the prime and target stimuli was the same
165 (e.g., both drifting rightward), referred to as *coherent prime* condition; and 2) the case in
166 which the prime and target stimuli had opposite directions (e.g., the prime drifting rightward
167 and the target drifting leftward), referred to as *incoherent prime* condition. The case in which
168 the prime stimulus drifted vertically (midpoint of the priming curve) will be referred to as
169 *neutral prime* condition. This terminology will be used for both the identity- and cross-
170 priming conditions and for both the P and G groups.

171 The first step in our analysis was to verify whether the prime stimuli were indeed
172 capable of biasing rat choices depending on the level of coherence between their direction
173 and that of the target stimuli, in case of the identity-priming condition. This was the case for
174 10 out of 11 rats of the G group and 9 out of 10 rats of the P group, which were therefore
175 included in the subsequent analysis (see Materials and Methods). For the G group, rat group
176 average accuracy at discriminating the motion direction of the target gratings was strongly
177 modulated, as function of the direction of the prime grating stimulus (Fig 2A, black curve). In
178 the coherent prime condition, rat classification of target direction was facilitated, as compared
179 to the reference neutral prime condition (dashed line). Conversely, in the incoherent prime
180 condition, rat classification accuracy was substantially lowered. Overall, the identity-priming
181 curve was approximately sigmoidal. Even for the P group, in the identity-priming condition, a
182 strong priming was observed (Fig 2B, black curve). Also in this case, the magnitude and sign

183 of the priming effect depended on the similarity between the directions of the prime and
184 target plaid stimuli, resulting in an approximately monotonic drop of rat classification
185 accuracy from the coherent priming condition towards the incoherent one.

186 The strong modulation of rat classification accuracy in the identity-priming condition
187 has two important implications. First, it demonstrates the effectiveness of the priming
188 paradigm in capturing the perceived similarity between the learned (horizontal) motion
189 directions of the target stimuli and the untrained (previously unseen) directions of the prime
190 stimuli, in the case in which targets and primes are either both gratings or both plaids (i.e.
191 *identity-priming* condition). Second, and more importantly, it serves as a reference against
192 which to compare the modulation of the accuracy observed in the cross-priming condition. In
193 fact, the degree of similarity between the priming curves measured in the identity- and cross-
194 priming conditions (i.e., between the black and gray curves in Fig 2) allows answering two
195 key questions about the neuronal representations of the grating and plaid stimuli.

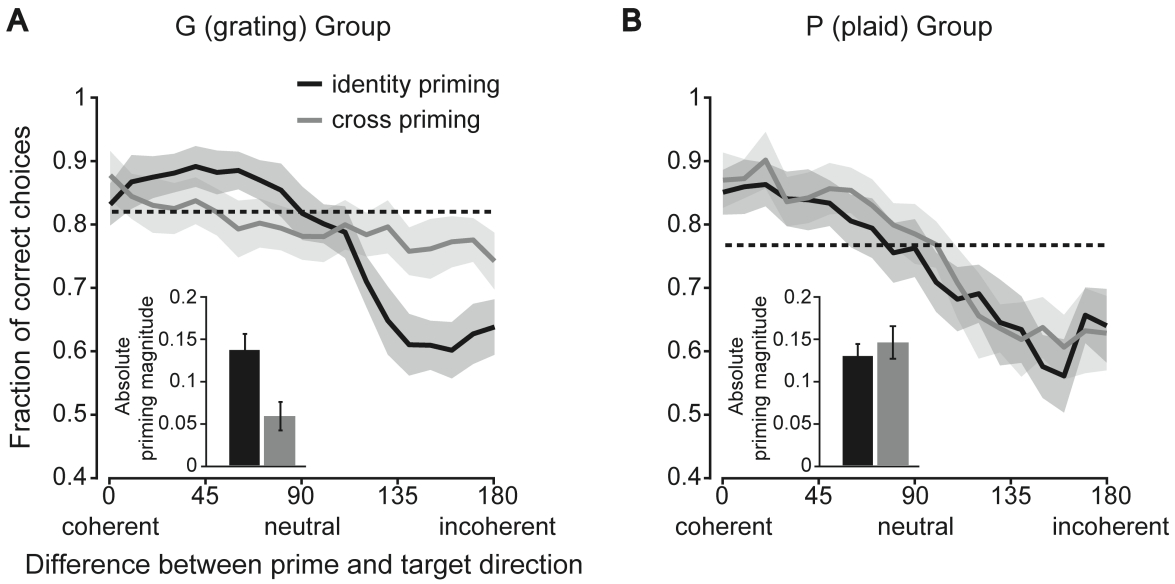

196

197 **Fig 2 – Identity- and cross-priming curves.** (**A**) The identity-priming curve (black) reports the mean
198 accuracy of the rats of the G group at discriminating the leftward from the rightward drifting gratings,
199 as a function of the difference between the direction of these target stimuli and the gratings that were

used as prime stimuli. The cross-priming curve (gray) reports rat mean accuracy when the plaids were used instead as prime stimuli. The shaded areas are 95% confidence intervals obtained by bootstrap (see Materials and methods). The dashed line shows the accuracy achieved with the neutral identity-prime stimulus (i.e., the grating drifting upward). The inset quantifies the absolute magnitude of priming obtained in the two cases, as the mean absolute difference between the four leftmost (and rightmost) points in a curve and the point corresponding to the neutral condition. The error bars show 95% confidence intervals obtained by bootstrap (see Materials and methods). (**B**) Same as in A, but for the rats of the P group. That is, in this case, the curves report rat mean accuracy at discriminating the leftward from the rightward drifting plaids. The identity-priming curve (black) refers to trials where the plaids were used as prime stimuli, while the cross-priming curve (gray) refers to trials where the gratings were used as primes.

Evidence of a shared representation of gratings' and plaids' motion direction

The first question is whether these representations are "shared" (i.e., the same neural population encodes both gratings and plaids) or "non-shared" (i.e., independent, non-overlapping populations represent the two types of stimuli). In the former case, we would expect a substantial modulation of rat classification accuracy also in the cross-priming condition, possibly as large as in the identity-priming condition. In the latter case, no cross-priming effect would be observable, given the independence of the two populations underlying the perception of gratings and plaids. In case of shared representations, then a second crucial question could be answered by comparing the shapes of the priming curves obtained in the identity- and cross-priming conditions. If rats spontaneously represented the stimuli according to their global direction, then the priming curves produced by gratings and plaids would be very similar, given that, by construction, the global direction of the prime stimuli was the same for matching grating and plaid primes. If the opposite were true, then the priming curves produced by gratings and plaids would be different.

226 In the G group (Fig 2A), the cross-priming curve (gray) was almost flat and
227 significantly different from the identity-priming curve (black), as shown by the non-
228 overlapping 95% confidence intervals (shaded areas). The priming magnitude produced by
229 the plaid stimuli was found to be significantly smaller than that produced by the gratings (Fig
230 2A, inset: gray vs. black bar; non-overlapping 95% confidence intervals). This inability of the
231 plaids (when used as prime stimuli) to affect the discrimination (hence the perception) of the
232 target gratings strongly suggests that, for the rats of the G group, the neuronal population
233 representing the direction of the gratings was largely inactive during the presentation of the
234 plaids.

235 By contrast, in the P group, the cross-priming and identity-priming curves largely
236 overlapped (Fig 2B: gray vs. black curve). As a result, the priming magnitude observed in the
237 two conditions was equally large (Fig 2B, inset: gray vs. black bar; overlapping 95%
238 confidence intervals). In other words, the gratings and plaids (when used as prime stimuli)
239 were equally effective at biasing rat discrimination of the target plaids. This indicates that the
240 same neuronal population was active during the presentation of both kinds of stimuli, as
241 expected in case of a shared representation of gratings and plaids. More importantly, the
242 priming produced by gratings and plaids was not only equivalent in terms of overall
243 magnitude, but it was also very similar for matching (global) directions of the two stimuli
244 (i.e., overlapping curves in Fig 2B). This strongly suggests that the representation of plaids in
245 rats trained to discriminate such stimuli (P group) is not only shared with the representation
246 of gratings, but is structured in such a way to encode plaids' global motion direction.

247 **Rat perception of drifting plaids is more consistent with a pattern- than a component-**
248 **based representation of motion signals**

249 To test more formally the extent to which the priming curves observed for the P group
250 are consistent with a representation of global motion direction of the plaid stimuli, we

performed a decoding analysis using linear classifiers. We simulated two alternative scenarios: a representation made of pattern cells (i.e., neurons tuned to the global direction of the plaids) and a representation made of component cells (i.e., neurons tuned to the local direction of the constituent gratings of the plaids).

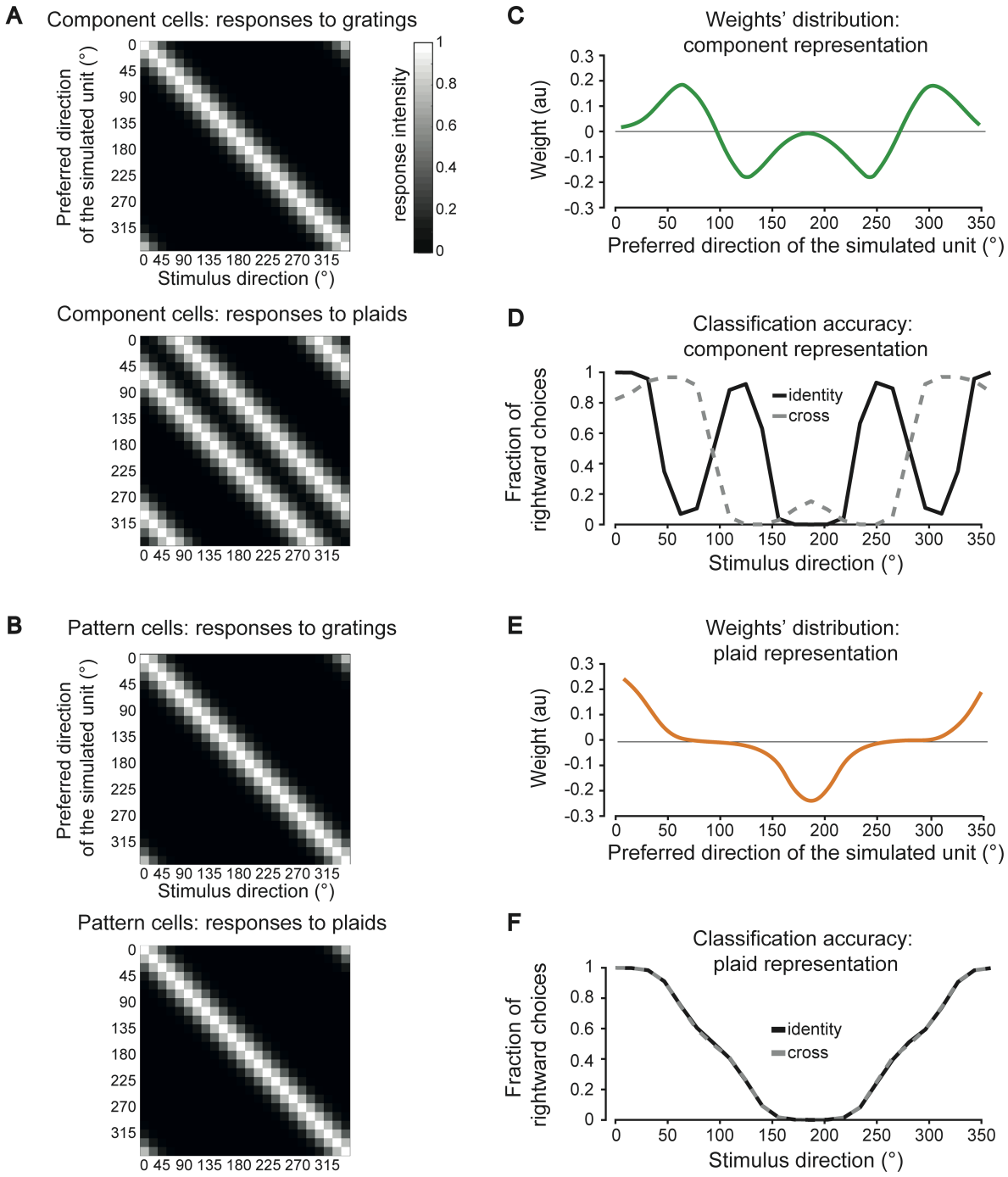

Fig 3 – Simulating the discrimination accuracy afforded by component- and a pattern-based representations. (**A**) Tuning curves (rows) for a simulated population of 24 components cells, whose preferred directions homogeneously spanned the [0º 360º] range, starting from 0º (first row), up to 345º (last row), in steps of 15º. The responses of the units are shown as a function of 24 possible directions (columns) of the grating (top) and plaid (bottom) stimuli. The gray scale bar indicates the intensity of the response. (**B**) Same as in A but for a population of 24 simulated pattern cells. (**C**) Weights assigned to each of the 24 component cells in A (the x axis reports the preferred direction of each unit) by a logistic classifier that was trained to discriminate a 0º- (rightward) from a 180º-drifting (leftward) plaid. (**D**) Fraction of times that the logistic classifier fed with the component-based representation (whose weights are shown in C) classified the test stimuli as drifting rightward (i.e., at 0º). The test stimuli were either plaids (solid black curve) or gratings (dashed gray curve) spanning the whole [0º 360º] range of directions. (**E**) Weights assigned to each of the 24 pattern cells in B by a logistic classifier that was trained to discriminate a 0º- (rightward) from a 180º-drifting (leftward) plaid. (**F**) Same as in D, but for the logistic classifier fed with the pattern-based representation (whose weights are shown in E). S1 Fig 1 reports an extended version of these simulations, where a range of widths of the tuning curves (from very broad to very narrow) was tested.

In both cases, we simulated a population of 24 units, whose preferred directions homogeneously spanned the [0º 360º] range (i.e., one unit tuned to every direction in steps of 15º; Fig 3A-B). The tuning curves of the simulated units were defined by Von Mises functions (46,47), which are the circular analog of Gaussian functions and whose width is controlled by the parameter k, which is equivalent to the inverse of the variance of a Gaussian distribution (48) (see Methods for details). In our simulations, k was set to 7, which roughly corresponds to a peak of the tuning curve with a full width at half maximum (FWHM) of about 50º (see grayscale matrix in Fig 3A-B). By construction, for a component cell, the response to the drifting plaids as a function of their direction featured two peaks, separated by 120º (Fig 3A, bottom). These peaks correspond to the global directions of the plaid that bring one of the constituent gratings to be aligned to the preferred (local) direction of the unit (i.e.,

284 the one shown in Fig 3A, top). Conversely, the tuning curves of the simulated pattern cells
285 featured a single peak, corresponding the global direction of the stimulus (no matter whether
286 grating or plaid) they were tuned to (Fig 3B) (see Methods for further details).

287 We used these populations to simulate how a rat trained to discriminate leftward from
288 rightward drifting plaids (i.e., same task of the animals in the P group; see Fig 1B) would
289 spontaneously categorize the novel, previously unseen gratings and plaids used as prime
290 stimuli, under the assumption of either a purely pattern-based or a purely component-based
291 representation. Rat perceptual decisions were simulated by training a logistic classifier to
292 discriminate the leftward from the rightward drifting plaids, based on their representation in
293 the simulated neural population space. As a result of the training, each classifier learned to
294 rely on a specific subset of the units of the representation, as shown by the weights'
295 distribution of Fig 3C and E. We then tested how each classifier categorized the sets of
296 drifting plaids and gratings used in the identity- and cross-priming experiments. This yielded
297 generalization curves (Fig 3D and F) that, in the [0º 180º] range, are equivalent to the
298 identity- and cross-priming curves of Fig 2B.

299 The shape of the generalization curves can be understood by considering the
300 corresponding weights' distribution resulting from training with the 0º- and 180º-drifting
301 plaids. In the case of the component representation, these training stimuli activated mostly the
302 units tuned for directions at ±60º with respect to the direction of the stimuli themselves. As a
303 result, the classifier learned to assign large, positive weights to the units tuned at ~60º and
304 ~300º (i.e., those providing the strongest evidence of a rightward, 0º-drifting plaid), and
305 large, negative weights to the units tuned at ~120º and ~240º (i.e., those providing the
306 strongest evidence of a leftward, 180º-drifting plaid) – hence, the twin positive and negative
307 peaks in the weights' distribution (Fig 3C).

308 When the classifier was presented with test plaids spanning the whole [0º 360º] range
309 of directions, the proportion of rightward choices (solid curve in Fig 3D) was obviously
310 maximal (i.e., 100%) at 0º (since this was the rightward training direction), but then dropped
311 quickly, becoming minimal (i.e., 0%) for a plaid drifting at 60º. In fact, for this stimulus, one
312 of the constituent gratings activated the units tuned at ~0º, where the weights were close to
313 zero (see Fig 3C), while the other grating activated the units tuned at ~120º, where the
314 weights were large but negative, since those units signaled the presence of the leftward, 180º-
315 drifting plaid. When the direction of the test plaid further increased, the proportion of
316 rightward choices grew again, reaching a new positive peak at 120º. This was because one of
317 the constituent gratings of the plaid activated the units tuned at 60º (with large, positive
318 weights), while the other grating activated those tuned at 180º (where the weights were close
319 to zero). The generalization curve reached again another minimum when the test plaid drifted
320 at 180º (the leftward training direction), with the constituent gratings that activated the units
321 tuned at 120º and 240º, with large, negative weights. As shown in Fig 3D, a mirror trend was
322 produced for plaids drifting along directions larger than 180º.

323 As for the generalization curve obtained when feeding to the classifier isolated
324 drifting gratings (dashed, gray curve in Fig 3D, which is equivalent to the cross-priming
325 curve of Fig 2B), it largely followed the shape of the weights' distribution. This can be easily
326 understood, given that a grating provided as much evidence of rightward (leftward) motion as
327 close its direction was to the positive (negative) peaks of the weights' distribution. As a
328 result, the generalization curves produced by plaids and gratings (solid vs. dashed curve in
329 Fig 3D) followed completely different trends, with no overlap. In addition, none of them
330 matched the monotonic decrease observed for the corresponding identity- and cross-priming
331 curves of Fig 2B (solid vs. dashed curve). Together, this strongly suggests that a

representation made of component cells is incompatible with the priming curves measured for the rats of the P group.

A very different result was found for the simulated representation of pattern cells. In this case, the weights' distribution had a large, positive peak at 0º, corresponding to the units coding for the rightward motion, as well as a large, negative peak at 180º, corresponding to the units coding for the leftward motion (Fig 3E). Given that, by construction, the pattern cells responded in the same way to isolated gratings and plaids having the same (global) direction, the generalization curves corresponding to the identity- and cross-priming conditions fully overlapped (Fig 3F, black, solid line vs. gray, dashed line). More importantly, they both followed a monotonic, decreasing trend in the [0º 180º] range, which largely trailed the shape of the weights' distribution. Crucially, these trends were highly consistent with those observed for the priming curves of Fig 2B. This shows that, differently from the case of the component representation, a representation made of pattern cells would support the identity- and cross-priming curves obtained for the rats of the P group.

To verify the extent to which this conclusion depended on the width of the tuning curves of the simulated units, we allowed the parameter k (that defines the width of the Von Mises functions) to range from 0.5 to 11. Examples of the resulting tuning curves obtained for the simulated component cells are shown in S1 Fig panel A. At very low k, as a result of the increased broadness of the tuning, the two peaks in the response to the plaid stimuli (solid curves) tended to merge. This translated in a broadening of the weights' distribution of the logistic classifier (S1 Fig panel B) and in a concomitant increase of the similarity between the generalization curves obtained for gratings and plaids (S1 Fig panel C; dashed vs. solid curves). To quantify this similarity, we computed the absolute differences between the proportions of rightward choices in the two generalization curves across all tested directions and we averaged them. The resulting average difference was large (as already shown in Fig

357 3D) for $k > 5$ but became negligible for $k < 3$ (S1 Fig panel D). This corresponds to peaks in
358 the tuning curves with FWHM ~ 80° or wider (see S1 Fig panel A). Therefore, a population
359 of component cells with such a broad tuning could in principle account for the overlapping
360 identity- and cross-priming curves obtained for the P group in our experiments (Fig 2B).

361 To understand whether this is a plausible scenario, one would need to measure the
362 width of tuning of component cells in rodent visual cortex. Unfortunately, the few studies
363 investigating component and pattern cells in mouse visual cortex did not perform a statistical
364 characterization of the sharpness of their orientation tuning. This prevented our simulated
365 units from quantitatively matching a physiological ground-truth in terms of orientation
366 tuning. Nevertheless, the tuning curves of the example component cells reported in rodent
367 studies investigating this topic feature such sharp and narrow peaks over the orientation axis
368 to decisively fall in the regime corresponding to $k >> 5$ in our simulations (i.e., with FWHM
369 << 60°) (16,17). A similar conclusion is supported by the general tendency of orientation
370 tuning to be quite sharp in mouse and rat visual cortex (47,49–55). As such, the most likely
371 hypothesis is that the stimulus representation underlying the priming curves of the P group
372 (Fig 2B) consisted of pattern, rather than component cells. Further neurophysiological studies
373 will be necessary to verify this hypothesis – e.g., by directly testing, as done here in our
374 simulations, the extent to which populations of recorded component and pattern cells yield
375 direction classification curves that are consistent with the priming curves measured in our
376 experiments.

377 **Summary of our findings**

378 The results presented in Fig 2B show that rats are capable of spontaneously combining local
379 motion cues into integrated percepts of global motion direction of a complex visual pattern.
380 Our simulations show that this ability is consistent with a representation of global motion
381 signals, as the one provided by pattern cells (Fig 3 and S1 Fig panel B). As such, our findings

strongly suggest that rats are capable of processing motion stimuli by relying on pattern-like representations. This, in turn, establishes a candidate perceptual correlate of the neuronal selectivity for global motion previously reported across rodent visual cortical areas (16–18), suggesting that, despite being a tiny fraction of the overall visual cortical population, rodent pattern cells do play an important (possibly preferential) role in the processing of visual motion. Critically, such motion integration ability only emerged in rats trained to discriminate the plaid stimuli (P group). The animals trained in the grating discrimination task (G group) were instead virtually insensitive to the plaids (Fig 2A), indicating that the neuronal population they relied upon to encode the gratings failed to effectively represent the plaids. In the following sections we provide two tentative explanations of such observations based on different sets of assumptions. Simulations of component- and pattern-based representations and linear read-out mechanisms (similar to those shown in Fig 3) allowed testing the ability of such assumptions to possibly explain our findings.

Simulating a scenario where training with either gratings or plaids leads to a decoding pool enriched of either component or pattern cells.

The first explanation rests on the hypothesis that the specific discrimination being reinforced during the training biased the recruitment of the visual cortical pool that was read out by downstream decision neurons towards either a more component-enriched or a more pattern-enriched cell population (referred to as the "decoding pool" in what follows). Such a task-dependent selection of the decoding pool may stem from differences between component and pattern cells in terms of two key properties: i) their relative proportion within visual cortex; and ii) the intensity of their responses to gratings and plaids.

With regard to the first property, although the number of studies investigating motion integration in rodent visual cortical areas is still limited (16–18), a finding that is consistent

among them is that component cells by far outnumber pattern cells, with the former being ~25% of direction-tuned units and the latter being about ~5% (with the rest being unclassified). With respect to the second property, a well-known phenomenon likely affecting the strength of grating and plaid responses is cross-orientation suppression (56–59), which has been recently documented also in rodents (43,60,61). It consists in a reduction of the response to the preferred oriented stimulus when this is presented together with other stimuli with different orientations. This means that cross-orientation suppression could, in principle, lead to diminished responses to plaids as compared to gratings. However, most studies documenting this phenomenon mainly targeted V1, without distinguishing between pattern and component cells. In addition, when focusing on studies of motion integration in rodents (16–18), it was difficult to draw any insight about the incidence of cross-orientation suppression in pattern and component cells, because of methodological limitations (e.g., tuning curves normalization and calcium imaging lacking spike-count-level information). This is why we turned to the primate literature, finding hints of cross-orientation suppression being stronger in component cells than in pattern cells (20,21).

Our hypothesis is that the combined effect of component cells being more numerous than pattern cells, but also more sensitive to cross-orientation suppression, led the decoding pool to become dominated by component cells in the case of training with gratings (G group) and by pattern cells in the case of training with plaids (P group). In turn, this would qualitatively explain the difference in terms of cross-priming found for the rats of the G and P groups (Fig 2), as graphically illustrated in Fig 4A, B. Briefly, in the case of training with gratings (Fig 4A, top), these stimuli would strongly activate both pattern (orange) and component (green) cells (filled and unfilled neurons indicate, respectively, responsive and unresponsive units). As such, the selection of the neuronal decoding pool by a downstream decision neuron would not be biased towards either class of neurons (because of no

differences in their responsiveness). However, since the component cells substantially outnumber the pattern cells, the decoding pool would contain more of the former (black-boundary neurons) than of the latter (red-boundary neurons). This follows from the assumption that the selection of the decoding pool is the result of a random sampling from the subpopulation of all responsive units. This, in turn, is consistent with the idea that such recruiting process is mediated by some form of plasticity similar to the reward-gated Hebbian learning reviewed in (62). In the priming experiment, all the neurons in the decoding pool would be active during presentation of the grating primes (Fig 4A, middle), leading to the strong identity priming observed in Fig 2A (solid curve). By contrast, most component cells in the pool would be strongly depressed by cross-orientation suppression during presentation of the plaid primes (Fig 4A, bottom; empty black-boundary neurons), and the few pattern cells in the pool (orange-filled, red-boundary neurons), although active, would not be enough to affect the perception of the target stimulus. Hence, the lack of cross-priming in the group of rats trained with gratings (Fig 2A, gray curve).

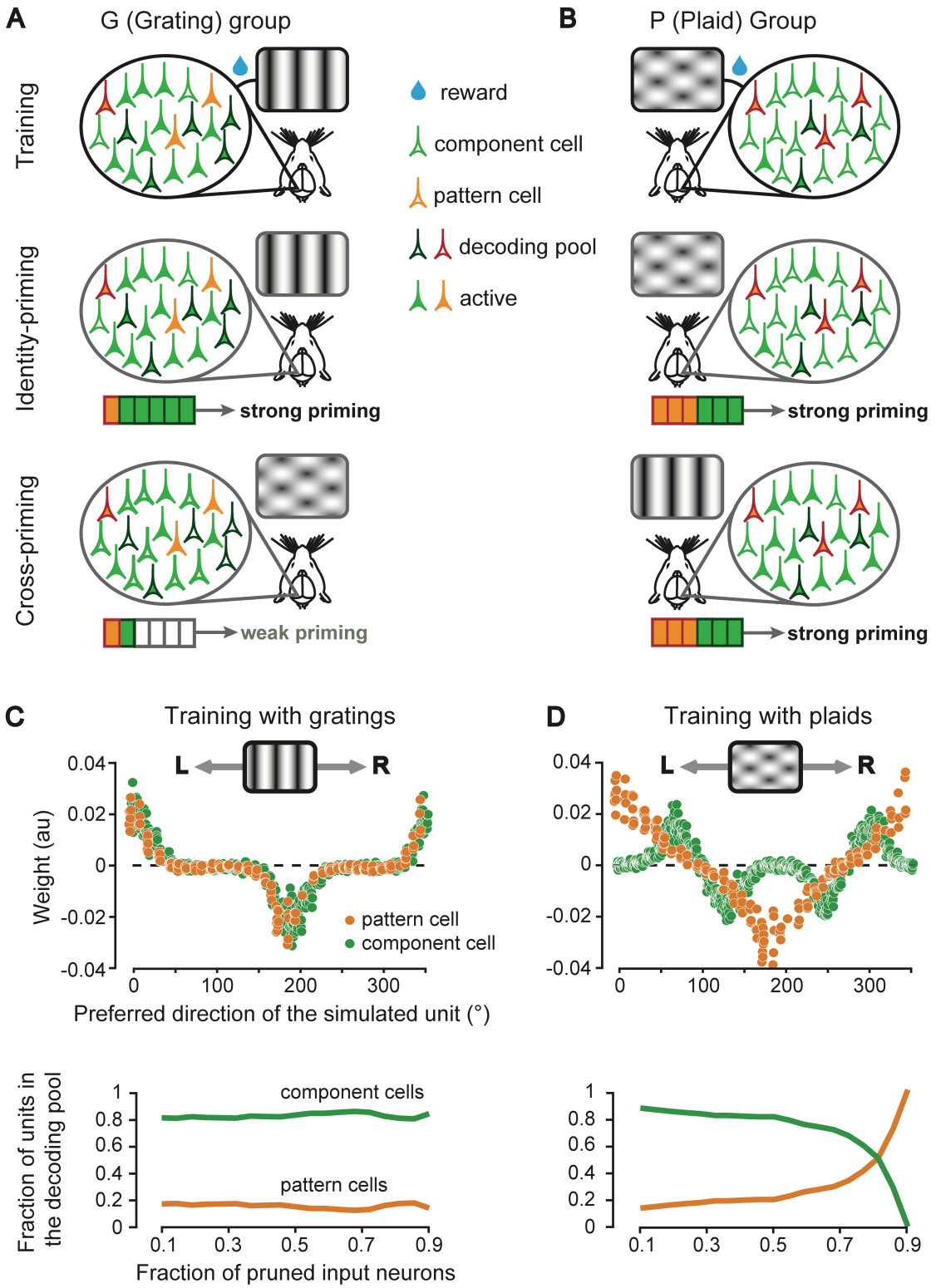

Fig 4 – Simulating a scenario where training with either gratings or plaids leads to a decoding pool enriched of either component or pattern cells. (**A**) Cartoon illustrating how training with gratings would lead to the selection of a decoding pool enriched of component cells, under the assumption that: 1) component cells are more numerous than pattern cells; and 2) cross-orientation

suppression is stronger for component than pattern cells. The sketched pyramidal neurons represent either component (green) or pattern (orange) cells. Filled and unfilled neurons indicate, respectively, responsive and unresponsive units. Black- and red-boundary neurons indicate the cells that the decision neuron learned to rely upon to discriminate the rightward- from the leftward-drifting gratings (i.e., the cells in the decoding pool). The grating stimuli activate equally strongly the component and pattern cells, but, being the former more numerous, the decoding pool is mainly composed of component cells (top). When tested with gratings, the cells in the decoding pool are strongly activated (middle), but, when they are tested with plaids, they are only weakly activated (bottom), because of cross-orientation suppression. (**B**) Cartoon illustrating how training with plaids would lead to the selection of a decoding pool enriched of pattern cells. Because of cross-orientation suppression, component cells are weakly activated by plaids, thus the decoding pool is enriched of pattern cells (top). As a result, the decoding pool is strongly activated when presented with both plaids (middle) or gratings (bottom). (**C**) Top: weights assigned to a mixed population of component (green) and pattern (orange) cells, as a function of their preferred direction, by a logistic classifier that was trained to discriminate a 0º- (rightward) from a 180º-drifting (leftward) grating. Bottom: The proportion of component (green) and pattern cells (orange), initially set to, respectively, 80% and 20% of the total, remained unchanged when weights with increasingly larger magnitude were progressively set to zero (i.e., pruned from the decoding pool). (**D**) Top: same as in C (top) but for a logistic classifier trained to discriminate a 0º- (rightward) from a 180º-drifting (leftward) plaid. Because of cross-orientation suppression, the classifier learned to assign weights with lower magnitude to the component cells. Bottom: as a result, when the input connections to the classifier were made increasingly sparser (by pruning weights with progressively larger magnitude), the proportion of pattern cells in the decoding pool (orange) reached and overtook the proportion of component cells (green).

In the case of training with plaids (Fig 4B, top), these stimuli would strongly activate the population of pattern cells (orange-filled neurons) but only weakly excite the component cells (green-filled neurons), because of cross-orientation suppression. This would lead to a strong bias towards the recruitment of pattern cells in the decoding pool (red-boundary neurons) by a downstream decision neuron. When tested with prime stimuli, such pattern-

479 enriched pool would respond with a similar intensity to both kinds of primes (grating and
480 plaids; Fig 4B, middle and bottom panels respectively), leading to similar priming curves in
481 both identity- and cross-priming conditions, as shown in Fig 2B (solid vs. gray curve). This
482 would account for the shared representation of global motion direction observed for rats
483 trained with plaids.

484 To quantitatively test whether the mechanistic account hypothesized in the previous
485 paragraphs could explain our findings, we built a computational model where a decision
486 neuron had to select his afferent units from a mixed population of component and pattern
487 cells, in order to discriminate the direction of either drifting gratings or plaids. The relative
488 proportion of simulated component (80%) and pattern (20%) cells roughly matched that
489 found, on average, across rodent visual areas V1, LM and RL (16–18). Each unit was
490 simulated as a Poisson spiking neuron, whose average firing rate as a function of direction
491 was defined by a von Mises function (46,47) having a peak that was randomly sampled
492 across the [0º 350º] direction axis (see Materials and methods for details).

493 In addition, to simulate cross-orientation suppression in component cells, their peak
494 responses to plaids were set to half their peak responses to gratings. On the other hand,
495 pattern cells were assumed to be unaffected by cross-orientation suppression. As for the
496 simulation of Fig 3, the decision neuron consisted in a logistic classifier that was trained to
497 discriminate between 0º- and 180º-drifting stimuli (i.e., leftward vs. rightward motion). This
498 classifier simply performed a weighted sum over the inputs provided by all the simulated
499 component and pattern cells, followed by the application of a sigmoidal nonlinearity. As a
500 result of training, the weights became adjusted in such a way to maximize the classification
501 accuracy (eventually attaining 100% in such a simple motion discrimination task).

502 When trained in the grating discrimination task (to simulate the training regime of the
503 G group), the classifier learned to rely more heavily on those motion detectors (no matter

504 whether component or pattern cells) whose preferred direction was close to that of the
505 training stimuli. This is shown in Fig 4C (top), where the weights of the simulated units as a
506 function of their preferred direction are reported. For both the component (green dots) and
507 pattern (orange dots) cell populations, the most informative neurons were those with
508 preferred direction close to 0º (rightward-drifting gratings) and 180º (leftward-drifting
509 gratings), while the units tuned around the vertical drift direction (i.e., 90º and 270º) were
510 assigned close-to-zero weights. Given these weight distributions, we simulated different
511 degrees of sparsity constraints on the connectivity of the decision neuron. This was done by
512 pruning input connections with progressively larger weight magnitude, thus gradually
513 reducing the size of the decoding pool. However, given the closely matching weight
514 magnitudes of the component and pattern cells, the level of pruning did not alter their relative
515 proportion in the decoding pool – this proportion remained the same as in the original
516 population (i.e., 80% vs. 20%; Fig 4C, bottom). This confirmed the intuition (see Fig 4A) that
517 training with gratings, even in presence of asymmetric cross-orientation suppression (i.e.,
518 affecting component but not pattern cells), leads to a decoding pool that simply reflects the
519 proportion of component and pattern cells of the overall cortical population and, as such, is
520 component-enriched.

521 A very different scenario emerged when we simulated the training of the P group in
522 the plaid discrimination task (see Fig 4D). The weight distribution learned by the classifier
523 for the pattern cell population (top, orange dots) was the same as in the grating discrimination
524 task. This is because our simulated pattern cells were by definition immune to cross-
525 orientation suppression. On the other hand, the weight distribution for the component cell
526 population (green dots) was very different from that obtained in the grating discrimination
527 task. First, since these cells responded to the components of the plaids (i.e., their constituent
528 gratings), the classifier learned to assign larger weights to those units with preferred direction

529 at ±60º (i.e., half plaid cross-angle) with respect to the global directions of the leftward- and
530 rightward-drifting plaids (same as for the simulations shown in Fig 3C). In addition, because
531 the simulated components cells were affected by cross-orientation suppression, the classifier
532 learned to rely less on component than on pattern cells, thus assigning lower weights to the
533 former than to the latter (compare the absolute height of the peaks in the distributions of
534 green and orange dots in Fig 4D, top). As a result, when the sparsity of the connections to the
535 decision neuron was increased, by leaving in the decoding pool only inputs with
536 progressively larger weight magnitude, the proportions of component and pattern cells in the
537 pool followed opposite, mirror trends (Fig 4D, bottom). While the former decreased (green
538 curve), the latter increased (orange curve), eventually leading to a reversal of the fraction of
539 component and pattern cells in the decoding pool when the decision neuron was pruned of
540 90% of its potential inputs. This confirmed the intuition (see Fig 4B) that cross-orientation
541 suppression can, at least in principle, strongly bias the recruitment of pattern cells in the
542 decoding pool, under the constraint of sparse connectivity to the decision neurons, thus
543 leading to a pattern-enriched representation despite the prevalence of component cells in the
544 overall cortical population. As a control experiment, we repeated the whole simulation
545 without any cross-orientation suppression. As expected, this yielded to a component-enriched
546 representation for both the simulated G and P groups (data not shown).

547 **Simulating a scenario where a decision neuron reading out a pattern representation**
548 **fails to be activated by plaids, if originally trained to discriminate drifting gratings.**

549 Despite the plausibility of the mechanism illustrated in the previous section, the key
550 assumption of having weaker cross-orientation suppression on pattern cells than on
551 component cells rests on hints from the primate literature only and has never been directly
552 demonstrated in rodents. In addition, in our simulations, the decision neurons drew their

553 inputs from a mixed population of pattern and component cells. That is, we assumed the
554 decision neuron to pool from different stages of a putative motion processing hierarchy.
555 Considering primates, this assumption is clearly at odd with the higher functional and
556 anatomical rank of MT, with respect to V1, along the dorsal stream (3,4). In the case of
557 rodents, it is still unclear whether a similar hierarchy of dorsal areas exists, but at least one
558 study has reported extra-striate area RL to be richer of pattern cells than V1 (16). In addition,
559 although an anatomical hierarchy of motion processing stages as structured as the one found
560 in primates may not exist in rodents, pattern cells distributed over striate and extrastriate
561 cortex could still sit above component cells along the functional motion processing chain. In
562 fact, pattern cells, given their ability to encode motion direction in a shape-independent way,
563 would behave as better motion detectors than component cells in virtually any visually
564 guided behavior. As such, motion information could still be preferentially routed from visual
565 cortical areas (e.g., V1, RL, LM) to higher-order decision centers (i.e., frontal and parietal
566 cortices) mainly via pattern cells. This possibility is consistent with the well-established
567 ability of distinct subpopulations, within mouse V1, to selectively make (receive) target-
568 specific projections with (from) downstream (upstream) areas (51,63–66). In addition, it is
569 consistent with a very recent study showing that multiple visual areas (V1, LM and AL) are
570 causally involved in coding stimulus orientation and contrast (67) – a demonstration that the
571 representation of key visual features is distributed among neuronal populations within distinct
572 visual areas.

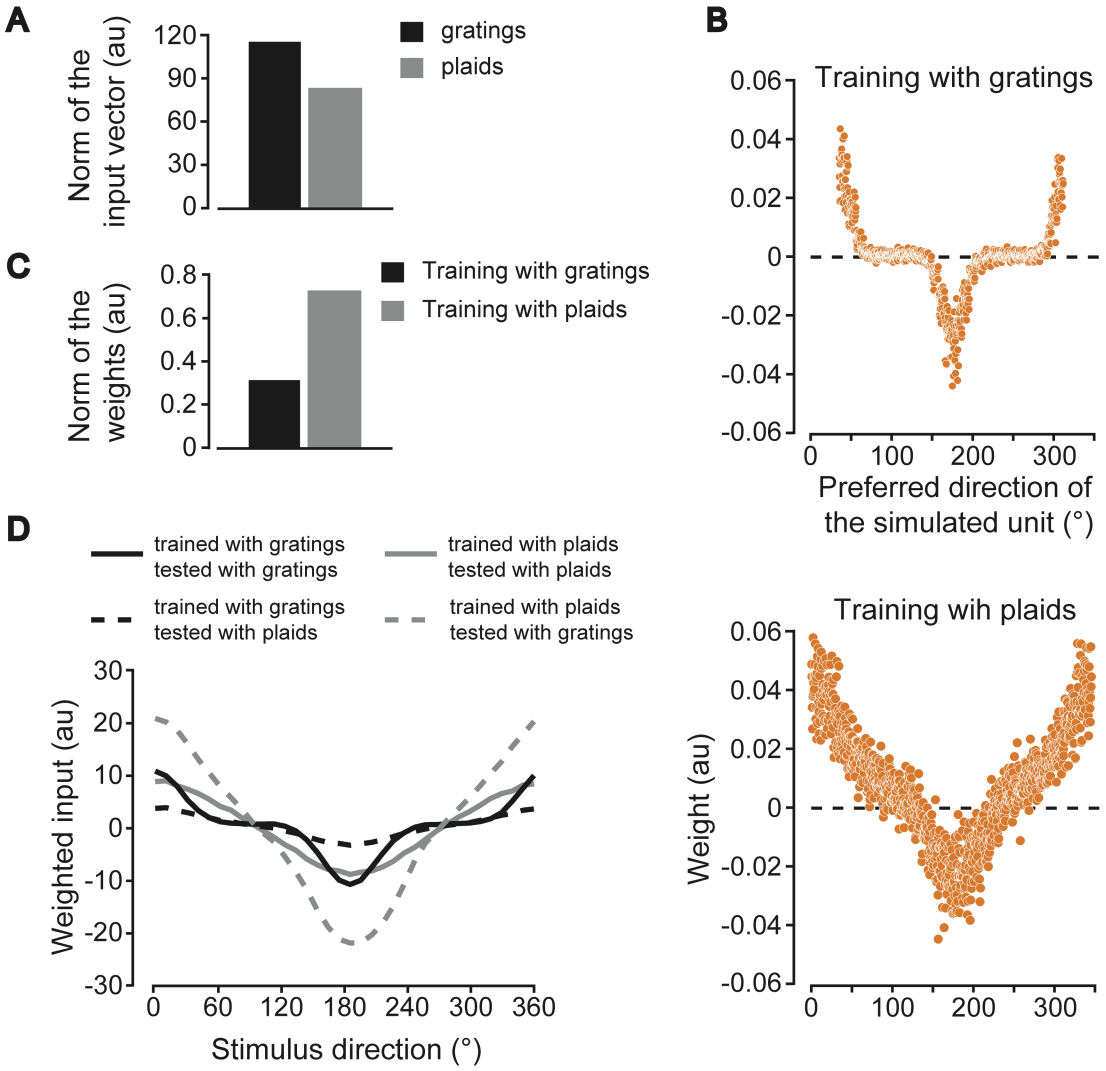

Fig 5 – Simulating a scenario where a decision neuron reading out a population of pattern cells fails to be strongly activated by drifting plaids, when originally trained to discriminate drifting gratings. (**A**) L2 norms of the population vectors fed as inputs to a decision neuron (simulated as a logistic classifier with L2 regularization) that was trained to discriminate either a 0º- from 180º-drifting grating (black) or a 0º- from 180º-drifting plaid (gray). The classifier received inputs from a population of pattern cells. Each bar reports the mean of the norms of the input populations vectors produced by the 0º- and 180º-drifting stimuli. (**B**) Weights assigned by the logistic classifier to the population of pattern cells as a function of their preferred direction, in case of training with gratings (top) and plaids (bottom). (**C**) L2 norms of the weights shown in B. (**D**) Weighted inputs to the logistic classifier, originally trained to discriminate either gratings (black curves) or plaids (gray curves), when the population of simulated pattern cells was presented with drifting stimuli, homogeneously spanning the

585 [0º 360º] range of directions. Such stimuli were either of the same kind (solid curves) or of a different
586 kind (dashed curves) of those used during training. For instance, a classifier originally trained with
587 plaids was tested with either plaids (gray, solid curve) or gratings (gray, dashed curve).
588

589 In light of these considerations, an alternative scenario to interpret our findings is one
590 where: i) decision neurons receive inputs mainly from pattern cells, regardless of the motion
591 discrimination task to be performed (i.e., the decoding pool is, by "construction", pattern
592 enriched); and ii) pattern cells are as sensitive to cross-orientation suppression as component
593 cells are. The question is whether these assumptions are consistent with the difference in the
594 magnitude of cross-priming produced by plaids on the rats of the G group (Fig 2A) and by
595 gratings on the rats of the P group (Fig 2B). To account for this difference, we reasoned that
596 pattern cells connected to a given decision neuron could fire less in response to plaids
597 (because of cross-orientation suppression) than in response to gratings. This could lead the
598 decision neuron to form stronger synaptic connections with its afferent pattern cells in the
599 case of training with plaids than with gratings, under the assumption that some compensatory
600 mechanisms actively keep the weighted input to the decision neuron around a target setpoint.
601 Such compensatory process would be fully consistent with the well-known role played by
602 homeostatic plasticity in cortex, where the overall synaptic strength scales as a function of the
603 magnitude of the input, so as to maintain the average firing rate of cortical neurons within a
604 given range (68–70).

605 To verify the plausibility of these intuitions, we simulated a downstream decision
606 neuron reading out the representation conveyed by a population of pattern cells with strong
607 cross-orientation suppression. As done in the previous section, we implemented the decision
608 neuron as a logistic classifier with a regularization term on the L2 norm of its "synaptic"
609 weights, so as to simulate the effect of homeostatic plasticity. The classifier was trained to

discriminate either gratings or plaids drifting in opposite directions (i.e., 0º vs. 180º motion direction). As a result of the cross-orientation suppression, the L2 norm of the population vectors fed as inputs to the classifier was larger for the gratings than for the plaids (Fig 5A). This led the magnitude of the weights to become larger in the case of training with the plaids than with the gratings (Fig 5B), with the L2 norm of the weights' vector being more than twice as large in the former case (Fig 5C).

This had the "homeostatic" effect of nearly equalizing the magnitude of the weighted inputs to the classifier, when this was fed with the same kind of stimuli that were used for training. As shown in Fig 5D, the weighted inputs resulting from presenting drifting gratings to the classifier that was trained to discriminate grating motion direction (solid black curve) were very close to the weighted inputs resulting from presenting drifting plaids to the classifier that was trained to discriminate plaid motion direction (solid gray curve). This would explain the strong identity priming observed for the rats of both the G and P groups in our experiment (Fig 2, black curves). At the same time, the large weights' magnitude resulting from the training with the plaids also guaranteed a very strong weighted input in the case of presentation of the grating stimuli (dashed gray curve in Fig 5D). This would explain the strong cross-priming observed for the rats of the P group (Fig 2B, gray curve). By contrast, the much smaller weights resulting from training with the gratings yielded a near-zero weighted input in the case of presentation of the plaid stimuli (dashed black curve in Fig 5D). This would explain the very small cross-priming observed for the rats of the G group (Fig 2A, gray curve). A plaid prime stimulus would simply be too weak (because of cross-orientation suppression) to activate the decision neuron through the weak, grating-adapted synaptic weights.

Conclusions and implications

Although speculative in nature, the two explanations detailed in the previous paragraphs and backed up by our simulations propose an account for the behavioral data reported in our study. Importantly, they both rest on well-defined physiological assumptions. As such, they give rise to alternative hypotheses about the neural mechanisms underlying the processing of motion information that could be tested experimentally. For instance, the first explanation (Fig 4) would be supported by observing cross-orientation suppression acting way more strongly on component than on pattern cells in rodent visual cortex. On the other hand, the second explanation (Fig 5) would be corroborated by observing that cross-orientation suppression affects equally strongly pattern and component cells, and by finding a projection-specific enrichment in the proportion of pattern cells relaying visual information to decision making centers, such as posterior parietal cortex (PPC) (29–32).

In conclusion, our study not only yields behavioral evidence of motion integration in rodents, but also provides solid grounding for future investigations aimed at dissecting the neuronal circuits underlying integration of local motion cues into global motion percepts. In fact, as highlighted in a recent perspective (71), a behavioral task involving direction discrimination of gratings and plaids is a necessary ingredient of future experiments aimed at establishing a correlational and/or causal link between pattern-like responses observed in rodent visual cortex and integrated motion perception.

Materials and methods

Animal procedures

We trained 21 male Long Evans rats (Charles River Laboratory) in a motion direction discrimination task. Upon arrival in the lab, rats weighed ~250 g, and they grew up to ~500 g.

658 Animals started training during ~ 7th postnatal week. During the experimental period, they
659 had free access to food, while their access to water was restricted. Their daily liquid intake
660 included 5 – 15 ml of a 1:4 juice-water solution, plus an ad libitum water access for one hour
661 after training. Training sessions lasted 50 – 70 minutes and took place 5 days per week. All
662 animal procedures were conducted in accordance with the international and institutional
663 standards for the care and use of animals in research and were approved by the Italian
664 Ministry of Health and after consulting with a veterinarian (Project DGSAF 25271, submitted
665 on December 1, 2014 and approved on September 4, 2015, approval 940/2015-PR).

666 **Behavioral apparatus and visual stimuli**

667 The behavioral rig consisted of two racks, each equipped with three operant boxes to allow
668 training a batch of six rats simultaneously (15,28). In each box, one of the walls bore a 3 cm-
669 diameter hole, so that a rat could extend its head outside the box and face the stimulus display
670 (a LCD monitor ASUS® Ve228 located at 30 cm from the viewing hole). The box was
671 equipped with three stainless-steel feeding needles (Cadence Science®), located right outside
672 the viewing hole, and serving as response ports and for reward delivery. To this end, each
673 needle was connected to a led-photodiode pair to detect when the nose of the animal
674 approached and touched it. The two ports positioned to the right and to the left of the hole
675 were connected to two computer-controlled syringe pumps (New Era Pump Systems NE-
676 500®) for delivery of liquid reward, while the central port served exclusively to trigger the
677 onset of each behavioral trial. Each rat learnt to extend its head through the viewing hole, lick
678 the central needle to trigger stimulus presentation and then lick either the left or right port to
679 report the identity of the visual stimulus presented in the current trial. In case of correct
680 response, the reward was delivered through the feeding needle. In case of an incorrect choice,
681 a 1-3 s timeout period started, with the stimulus display flickering from black to middle gray
682 at a rate of 15 Hz (during this period, a "failure" sound was also played). Stimulus

683 presentation, response collection and reward delivery were controlled via workstations
684 running open source MWorks software (https://mworks.github.io/).

685 As explained in the Results, the rats were divided in two groups. The animals in the G
686 group were trained to discriminate gratings drifting horizontally in opposite directions, i.e.,
687 180° (leftward) vs. 0° (rightward). The rats of the P group were trained to discriminate two
688 drifting plaids, whose global motion direction was, again, either 180° or 0º. The grating
689 stimuli consisted in full-field, full-contrast, sine wave drifting gratings with a temporal
690 frequency of 2 Hz and a spatial frequency of 0.04 cycles/°. The plaid stimuli were
691 constructed by superimposition of two half-contrast gratings (again 0.04 cycles/° and 2 Hz)
692 with a motion direction difference of 120° (i.e., 120° plaid cross-angle). In the experiments
693 with the priming paradigm (see below), the drift direction of the prime stimuli (either gratings
694 or plaids) was randomly sampled in each trial from 19 possible directions (i.e., from 0° to
695 180° in steps of 10; see Fig 1).

696 **Experimental design - Training phase**

697 As soon as a rat licked the central response port, the target stimulus appeared (either a grating
698 or a plaid depending on the animal's experimental group) and remained on screen for 2 s. To
699 prevent rats from making very quick, impulsive responses, a trial was aborted if the animal's
700 reaction time was lower than 300 ms. In such a case, the animal's response was not evaluated
701 (neither reward or time-out was administered), the stimulus was immediately turned off, and
702 a brief tone was played. Such "too fast" trials were also excluded from the analysis.
703 Similarly, trials in which the rat responded more than 2 s after the offset of the stimulus were
704 considered "ignored" and excluded from the analysis. No reward was delivered in these
705 invalid trials. In order to accomplish the task and receive the reward, the rat had to reach and
706 lick the response port matching the global motion direction of the target stimulus. Correct

707 execution of such task was rewarded equally for both directions during each experimental
708 session. In correct trials, the target stimulus remained on the screen for the whole reward
709 delivery period, so as to strengthen the operant association between stimulus response and
710 reward. On the other hand, when the animal provided an incorrect response, reward was not
711 delivered, the stimulus was immediately turned off and the timeout period started (see
712 previous section).

713 **Experimental design - Priming paradigm**

714 In the priming paradigm, a prime stimulus was shown to the animal before the target
715 stimulus. The prime duration was 75 ms, the inter-stimulus interval (ISI, i.e., the interval
716 separating the offset of the prime from the onset of the target) was also 75 ms and the target
717 duration was 750 ms. As in the training phase, "too fast" or "ignored" trials were excluded
718 from the analysis. Only, a trial was defined as "ignored" if the rat responded more than 1 s
719 after the onset of the target stimulus. As a result, the allowed response window extended from
720 300 to 1000 ms from target onset. As in the training phase, an animal, in order to obtain the
721 reward, had to reach and lick the response port (right or left) corresponding to the global
722 motion direction of the target. Accordingly, no feedback was ever provided to the rat
723 regarding the motion direction of prime stimuli. In this paradigm, the target was not kept on
724 screen during the reward, because there was no longer any need to favor the association
725 between response, stimulus, and reward. Only animals maintaining a performance in the
726 training task greater that 75% for 4 consecutive days were tested with this priming paradigm.

727 The rationale of this design rests on well-established findings in the human
728 psychophysics literature (42,72–74), where presenting an "adapter" before a "test" stimulus
729 has been shown to bias the perception of the test, depending on two key factors: the duration
730 of the adapter and the inter stimulus interval (ISI) between adapter and target presentation.

731 When the bias induced by the adapter attracts the perceptual choices towards the identity of
732 the adapter itself, this effect is called "priming". Vice versa, when it repels the perceptual
733 choices away from the identity of the adapter, it is named "adaptation after-effect". Our
734 group previously shown that brief presentation of a static shape (~50 ms), followed by a short
735 ISI (66 ms), is able to induce a strong and robust priming effect on rat response to a target
736 shape (27). Here, we adapted this paradigm to moving stimuli, and we relied on previous
737 motion priming studies in humans (42) to select the timing parameters of the task, in the
738 attempt of inducing a strong priming effect.

739 **Analysis of behavioral data**

740 Only rats displaying a strong identity-priming effect where included in the analysis described
741 in the main text. Quantitatively, this corresponded to setting a threshold on the absolute
742 priming magnitude in the identity priming condition amounting to 5%. Priming magnitude
743 was computed averaging together the mean values of the absolute difference between the left
744 and right extremes (4 points per side) of each priming curve with respect to the neutral prime
745 condition (insets in Fig 2). The enforcement of such criterion led to the rejection of one rat
746 per group, bringing the number of rats included in the analysis to 10 animals for the G group
747 and to 9 animals for the P group out of the original 11 animals trained in grating direction
748 discrimination and 10 trained in plaid direction discrimination.

749 To statistically compare the identity- and cross-priming curves obtained for each
750 group of rats (solid and dashed curves in Fig 2) we performed a bootstrap analysis, in which
751 the recorded behavioral sessions were resampled 50 times with replacement for each animal
752 independently. This gave us the possibility to estimate a bootstrap standard deviation for both
753 the average identity- and cross-priming curves of Fig 2, as well as for the average priming
754 magnitudes computed as described above (insets in Fig 2). Bootstrap standard deviations

755 were then used to compute normal 95% confidence intervals for the aforementioned
756 quantities (displayed in Fig 2 as shaded regions around the priming curves and as error bars
757 in the bar plot shown in the insets) (75). In computing confidence intervals for the 19 points
758 of a priming curve, the critical value corresponding to the chosen confidence level was
759 adjusted for multiple comparisons using Bonferroni correction.

760 **Computational modeling**

761 To interpret the results of our psychophysical tests, we simulated a decision neuron reading
762 out the activity of a simulated population of either component or pattern cells fed with either
763 grating or plaid stimuli. Three different simulations were performed to test the consistency of
764 our findings with three possible scenarios concerning the tuning of rat visual neurons for
765 motion direction and the choice of the decoding pool by the decision neuron. These
766 simulations have been already described in the Results and in the legends of Figs 3, 4 and 5.
767 Below, we explain some additional technical details about how we modeled the populations
768 of simulated component and pattern cells and how we implemented the logistic classifier
769 used to simulate the decision neuron.

770 *Simulations to check the consistency of the priming curves observed for the P group with a*
771 *pattern-based representation of global motion direction*

772 To check whether the shape of the priming curves observed for the rats of the P group (Fig
773 2B) was more consistent with a component-like or a pattern-like representation, we trained a
774 logistic classifier to solve the same motion discrimination task that was administered to the
775 rats (i.e., 0º- vs. 180º-drifting plaids), based on the responses of a simulated population of
776 either component of pattern cells (Fig 3). We then tested how the trained classifier would
777 decode the full range of drifting plaids and gratings used to obtain, respectively, the identity-
778 and cross-priming curves in Fig 2B. To simulate the tuning for local and global motion

779 direction of the populations of component and pattern cells, we used 24 Von Mises functions
780 (46,47) centered at equispaced angles along the circle (spaced by 15°). The von Mises
781 functions, which are the circular analogs of Gaussian functions, have a width that is
782 controlled by the parameter *k*, which, in turn, is equivalent to the inverse of the variance of a
783 Gaussian distribution (48). The peak value of the functions (and thus of the tuning curves)
784 was set to 1 for all the simulated units.

785 For a pattern cell, the simulated tuning curve was the same regardless of whether the
786 input stimulus was a plaid or a grating stimulus (compare matching rows in the top and
787 bottom panels of Fig 3B). That is, by construction, each simulated pattern cell responded to
788 the global direction of the plaid stimuli. Conversely, for a component cell, the simulated
789 tuning curve was defined by a single Von Mises function in case of presentation of the
790 grating stimuli (Fig 3A, top), but was defined by the superimposition of two von Mises
791 functions (with the peaks being 120º apart) in case of presentation of the plaid stimuli (Fig
792 3A, bottom). That is, by construction, each simulated component cell responded to the local
793 directions of the constituent gratings of the plaid stimuli, rather than to the global direction of
794 the plaid. For both the simulated pattern and component cells, the Von Mises functions were
795 summed to a constant background activity. In addition, to emulate the variability of neuronal
796 firing in response to identical stimuli, in each simulated trial, the actual response to a given
797 stimulus was affected by Gaussian noise with zero mean and $\sigma = 0.25$. The *k* parameter of the
798 Von Mises functions of the simulated pattern and component cells was set to 7 in the mean
799 simulation shown in Fig 3, while it was allowed to range between 0.5 and 11 in the more
800 extended simulations of S1 Fig. The ratio between the peak of the tuning curves and the
801 background rate was set to 10.

802 To model the training received by the rats in our experiment, we sampled for 500
803 times the responses of the whole population of either pattern or component cells to each of

804 the 0º- and 180º-drifting stimuli (either grating or plaids) used during the training phase. We
805 then trained a logistic regression classifier to discriminate the two sets of 0º and 180º
806 responses using gradient descent (implemented by the Matlab function "fminunc") and
807 including and L2 regularization term in the cost function (whose parameter lambda was set to
808 1). The weights resulting from such training are those shown in Fig 3C and E. Finally, we fed
809 to the classifier grating and plaid stimuli spanning the full range of possible global motion
810 directions (from 0º to 345º in steps of 15º) and we plotted the probability for each class of
811 stimuli to be classified as moving rightward as a function of its direction (Fig 3D and F).

812 *Simulations to explore the mechanisms that could lead to a strong cross-priming only in case*
813 *of training with plaid stimuli – scenario #1*

814 To obtain a proof of principle that the mechanisms illustrated in Fig 4A, B could lead to a
815 decoding pool enriched of pattern cells in case of training with plaids, we carried out a
816 second simulation. As before, we trained a logistic regression classifier in the same motion
817 direction discrimination task that was administered to our animals. This time, however, the
818 response properties of the simulated component and pattern cells, as well as their relative
819 proportion, better matched either the known properties derived from the rodent literature (16–
820 18) or those inferred based on the monkey literature (20,21). First, the simulated population
821 of pattern and component cells was much larger (i.e., 1000 units). It was composed of
822 Poisson firing neurons with either "component" or "pattern" tuning curves, built in the same
823 way as described in the previous section. Second, their proportion was 80% and 20%
824 respectively, so as to match the highest ratio of pattern to component cells observed in rodent
825 visual cortex (16). As in the previous simulation, we used Von Mises functions to define the
826 tuning curves of component and pattern cells (see description in the previous section). In this
827 case however, the preferred directions of the simulated neurons were not equispaced but
828 drawn randomly from a uniform distribution over the circle. Baseline value of tuning curves

829 was set to 2 spikes/second. Von Mises function of random amplitude (normally distributed
830 around 8 spikes/s with standard deviation of 1 spike per second) were added to this baseline.
831 The firing rate of the units in each trial was drawn from a Gaussian distribution with mean
832 equal to the value set by the tuning curves and standard deviation of 2 spikes/s. The width
833 (i.e., the parameter *k*; see previous paragraph) of the Von Mises functions was adjusted in
834 such a way that the Orientation Selectivity Index (OSI) of the resulting population of
835 component cells was distributed according to a Gaussian with a mean of 0.7 and a standard
836 deviation of 0.1, while the Direction Selectivity Index (DSI) was distributed according to a
837 Gaussian with a mean of 0.6 and a standard deviation of 0.2. OSI and DSI are standard
838 measures of orientation and direction tuning, whose definition can be found, for instance, in
839 (47,50,53,55).

840 To account for the imperfect cross-angle invariance documented by (17) we enlarged
841 the width of Von Mises functions used to simulate the tuning of pattern cells to plaids by
842 dividing the *k* parameter previously used to define their tuning to gratings (see previous
843 paragraph) by a factor 4. This made the responses of our simulated pattern cells better
844 matched to the known properties of mouse pattern cells, reproducing their tendency to have
845 broader tuning curves when tested with plaids than with gratings, especially when the plaids
846 have a large cross-angle (such as the one used in our study, i.e. 120°).

847 Finally, we simulated cross-orientation suppression in component cells – that is, we
848 imposed that the peak responses of component cells to the plaids were half of their peak
849 responses to the gratings, while pattern cells were implemented as being fully unaffected by
850 cross-orientation suppression (i.e., same peak responses to plaids and gratings). This scenario
851 was simulated because our goal was to test the hypothesis that, if cross-orientation
852 suppression affected strongly component cells but not pattern cells, then the decision neuron

853 would learn to preferentially connect with the latter, in the case of training with the plaid
854 stimuli.

855 To model the training received by the rats in our experiment, we sampled for 200
856 times the responses of the mixed population of pattern or component cells to each of the 0º-
857 and 180º-drifting stimuli (either grating or plaids) used during the training phase. We then
858 trained a logistic regression classifier to discriminate the two sets of 0º and 180º responses
859 using gradient descent (implemented by the Matlab function "fminunc") and including and
860 L2 regularization term in the cost function (whose parameter lambda was set to 1). The
861 weights resulting from such training are those shown in Fig 4C and D (top). Finally, we
862 simulated a scenario where, as a result of this training, the decision neuron would maintain
863 only the strongest of its synaptic connections with sensory neurons encoding the drifting
864 stimuli. To incorporate this sparseness constraint on the connectivity of the decision neuron,
865 we progressively pruned the weakest synaptic weights by applying a quantile-based
866 thresholding to their magnitude after training (i.e., by setting to zero any weight below the
867 chosen quantile of the original weight magnitude distribution). We then quantified the
868 proportion of pattern and component cells that survived the pruning and remained in the
869 decoding pool of the decision neuron as a function of the quantile used as a threshold (Fig 4C
870 and D, bottom). As a control, the whole simulation was also run without incorporating cross-
871 orientation suppression in the responses of component cells.

872 *Simulations to explore the mechanisms that could lead to a strong cross-priming only in case*
873 *of training with plaid stimuli – scenario #2*

874 Here, we simulated an alternative scenario where a decision neuron (modeled, again, as a
875 logistic classifier) is connected to a pool of sensory neurons made exclusively of pattern cells
876 that are strongly affected by cross-orientation suppression. As such, the parameters of the

simulations were the same as those described in the previous section, with only two notable differences: 1) no component cells were included in the decoding pool, but only pattern cells; 2) cross-orientation suppression affected pattern cells instead of components cells, and its impact was twice as strong as that of the previous stimulation (i.e., peak responses to plaids were 25% of peak responses to gratings). The training of the classifier was the same as described in the previous section. Note that the L2 regularization term in the cost function played the role of a homeostatic constraint on the overall weights' magnitude. Again, we compared the weights' distributions resulting from training with plaids and gratings (Fig 5B) and we also quantified the magnitude of weighted input (i.e., sensory "evidence") to the decision neuron, depending on the training and prime stimuli (Fig 5D).

Acknowledgments. We thank Daniele Bertolini for his help in developing and building the rigs for the behavioral experiments, and we thank Sofia Erica Rossi and Marco Salluzzo for their help in training rats in the motion discrimination task.

References

1. Lisberger SG. Visual Guidance of Smooth Pursuit Eye Movements. Annu Rev Vis Sci. 2015;1(1):447–68.
2. Nishida S, Kawabe T, Sawayama M, Fukiage T. Motion Perception: From Detection to Interpretation. Annu Rev Vis Sci. 2018;4(1):501–23.
3. Born RT, Bradley DC. Structure and function of visual area MT. Annu Rev Neurosci. 2005;28:157–89.
4. Orban GA. Higher Order Visual Processing in Macaque Extrastriate Cortex. Physiol Rev. 2008 Jan 1;88(1):59.
5. Adelson EH, Movshon JA. Phenomenal coherence of moving visual patterns. Nature. 1982 Dec;300(5892):523–5.

6. Fennema CL, Thompson WB. Velocity determination in scenes containing several moving objects. Comput Graph Image Process. 1979 Apr;9(4):301–15.

7. Wuerger S, Shapley R, Rubin N. "On the Visually Perceived Direction of Motion" by Hans Wallach: 60 Years Later. Perception. 1996 Nov;25(11):1317–67.

8. Marr D. Vision: a computational investigation into the human representation and processing of visual information. Cambridge, Mass: MIT Press; 2010. 403 p.

9. Fenno L, Yizhar O, Deisseroth K. The Development and Application of Optogenetics. Annu Rev Neurosci. 2011;34(1):389–412.

10. Chen T-W, Wardill TJ, Sun Y, Pulver SR, Renninger SL, Baohan A, et al. Ultrasensitive fluorescent proteins for imaging neuronal activity. Nature. 2013;499(7458):295.

11. Madisen L, Garner AR, Shimaoka D, Chuong AS, Klapoetke NC, Li L, et al. Transgenic mice for intersectional targeting of neural sensors and effectors with high specificity and performance. Neuron. 2015;85(5):942–58.

12. Luo L, Callaway EM, Svoboda K. Genetic Dissection of Neural Circuits. Neuron. 2008 Mar 13;57(5):634–60.

13. Luo L, Callaway EM, Svoboda K. Genetic Dissection of Neural Circuits: A Decade of Progress. Neuron. 2018 Apr 18;98(2):256–81.

14. Carandini M, Churchland AK. Probing perceptual decisions in rodents. Nat Neurosci. 2013 Jul;16(7):824–31.

15. Zoccolan D. Invariant visual object recognition and shape processing in rats. Behav Brain Res. 2015 May 15;285:10–33.

16. Juavinett AL, Callaway EM. Pattern and Component Motion Responses in Mouse Visual Cortical Areas. Curr Biol. 2015 Jun 29;25(13):1759–64.

17. Palagina G, Meyer JF, Smirnakis SM. Complex Visual Motion Representation in Mouse Area V1. J Neurosci. 2017 Jan 4;37(1):164–83.

18. Muir DR, Roth MM, Helmchen F, Kampa BM. Model-based analysis of pattern motion processing in mouse primary visual cortex. Front Neural Circuits [Internet]. 2015 Aug 5 [cited 2017 Apr 24];9. Available from: http://www.ncbi.nlm.nih.gov/pmc/articles/PMC4525018/

19. Simoncelli EP, Heeger DJ. A model of neuronal responses in visual area MT. Vision Res. 1998;38(5):743–61.

20. Smith MA, Majaj NJ, Movshon JA. Dynamics of motion signaling by neurons in macaque area MT. Nat Neurosci. 2005 Feb;8(2):220–8.

21. Rust NC, Mante V, Simoncelli EP, Movshon JA. How MT cells analyze the motion of visual patterns. Nat Neurosci. 2006 Nov;9(11):1421–31.

938 22. Solomon SS, Tailby C, Gharaei S, Camp AJ, Bourne JA, Solomon SG. Visual motion
939 integration by neurons in the middle temporal area of a New World monkey, the
940 marmoset: Pattern motion sensitivity in middle temporal area of marmosets. J Physiol.
941 2011 Dec;589(23):5741–58.

942 23. Douglas RM, Neve A, Quittenbaum JP, Alam NM, Prusky GT. Perception of visual
943 motion coherence by rats and mice. Vision Res. 2006 Sep 1;46(18):2842–7.

944 24. Stirman JN, Townsend LB, Smith SL. A touchscreen based global motion perception task
945 for mice. Vision Res. 2016 Oct 1;127(Supplement C):74–83.

946 25. Samonds JM, Lieberman S, Priebe NJ. Motion Discrimination and the Motion Aftereffect
947 in Mouse Vision. eNeuro. 2018 Dec;5(6).

948 26. Marques T, Summers MT, Fioreze G, Fridman M, Dias RF, Feller MB, et al. A Role for
949 Mouse Primary Visual Cortex in Motion Perception. Curr Biol CB. 2018
950 04;28(11):1703-1713.e6.

951 27. Tafazoli S, Di Filippo A, Zoccolan D. Transformation-Tolerant Object Recognition in
952 Rats Revealed by Visual Priming. J Neurosci. 2012 Jan 4;32(1):21–34.

953 28. Zoccolan D, Di Filippo A. Chapter 5 - Methodological Approaches to the Behavioural
954 Investigation of Visual Perception in Rodents. In: Ennaceur A, de Souza Silva MA,
955 editors. Handbook of Behavioral Neuroscience. Elsevier; 2018. p. 69–101. (Handbook
956 of Object Novelty Recognition; vol. 27).

957 29. Nikbakht N, Tafreshiha A, Zoccolan D, Diamond ME. Supralinear and Supramodal
958 Integration of Visual and Tactile Signals in Rats: Psychophysics and Neuronal
959 Mechanisms. Neuron. 2018 Feb 7;97(3):626-639.e8.

960 30. Licata AM, Kaufman MT, Raposo D, Ryan MB, Sheppard JP, Churchland AK. Posterior
961 Parietal Cortex Guides Visual Decisions in Rats. J Neurosci. 2017 May
962 10;37(19):4954–66.

963 31. Odoemene O, Pisupati S, Nguyen H, Churchland AK. Visual Evidence Accumulation
964 Guides Decision-Making in Unrestrained Mice. J Neurosci. 2018 Nov
965 21;38(47):10143–55.

966 32. Raposo D, Kaufman MT, Churchland AK. A category-free neural population supports
967 evolving demands during decision-making. Nat Neurosci. 2014 Dec;17(12):1784–92.

968 33. Stahl JS. Using eye movements to assess brain function in mice. Vision Res. 2004
969 Dec;44(28):3401–10.

970 34. Smith AT, Harris LR. Use of plaid patterns to distinguish the corticofugal and direct
971 retinal inputs to the brainstem optokinetic nystagmus generator. Exp Brain Res
972 [Internet]. 1991 Sep [cited 2019 Nov 23];86(2). Available from:
973 http://link.springer.com/10.1007/BF00228955

974 35. Harvey RJ, De'sperati C, Strata P. The Early Phase of Horizontal Optokinetic Responses
975 in the Pigmented Rat and the Effects of Lesions of the Visual Cortex. Vision Res. 1997
976 Jun;37(12):1615–25.

36. Newsome W, Pare E. A selective impairment of motion perception following lesions of the middle temporal visual area (MT). J Neurosci. 1988 Jun 1;8(6):2201–11.

37. Salzman CD, Britten KH, Newsome WT. Cortical microstimulation influences perceptual judgements of motion direction. Nature. 1990 Jul;346(6280):174–7.

38. Djurdjevic V, Ansuini A, Bertolini D, Macke JH, Zoccolan D. Accuracy of Rats in Discriminating Visual Objects Is Explained by the Complexity of Their Perceptual Strategy. Curr Biol. 2018 Apr 2;28(7):1005-1015.e5.

39. Alemi-Neissi A, Rosselli FB, Zoccolan D. Multifeatural Shape Processing in Rats Engaged in Invariant Visual Object Recognition. J Neurosci. 2013 Apr 3;33(14):5939–56.

40. Rosselli FB, Alemi A, Ansuini A, Zoccolan D. Object similarity affects the perceptual strategy underlying invariant visual object recognition in rats. Front Neural Circuits. 2015;9:10.

41. Zoccolan D, Oertelt N, DiCarlo JJ, Cox DD. A rodent model for the study of invariant visual object recognition. Proc Natl Acad Sci U A. 2009 May 26;106(21):8748–53.

42. Kanai R, Verstraten FAJ. Perceptual manifestations of fast neural plasticity: Motion priming, rapid motion aftereffect and perceptual sensitization. Vision Res. 2005 Nov;45(25–26):3109–16.

43. Alwis DS, Richards KL, Price NSC. Masking reduces orientation selectivity in rat visual cortex. J Neurophysiol. 2016 Nov 1;116(5):2331–41.

44. Dell KL, Arabzadeh E, Price NSC. Human-like perceptual masking is difficult to observe in rats performing an orientation discrimination task. PLOS ONE. 2018 Nov 21;13(11):e0207179.

45. Dell KL, Arabzadeh E, Price NSC. Differences in perceptual masking between humans and rats. Brain Behav. 2019;9(9):e01368.

46. Kohn A, Movshon JA. Adaptation changes the direction tuning of macaque MT neurons. Nat Neurosci. 2004 Jul;7(7):764–72.

47. Matteucci G, Marotti RB, Riggi M, Rosselli FB, Zoccolan D. Nonlinear Processing of Shape Information in Rat Lateral Extrastriate Cortex. J Neurosci. 2019 Feb 27;39(9):1649–70.

48. Berens P. CircStat: A MATLAB Toolbox for Circular Statistics. J Stat Softw. 2009;31(10).

49. Girman SV, Sauvé Y, Lund RD. Receptive Field Properties of Single Neurons in Rat Primary Visual Cortex. J Neurophysiol. 1999 Jul 1;82(1):301–11.

50. Niell CM, Stryker MP. Highly selective receptive fields in mouse visual cortex. J Neurosci. 2008 Jul 23;28(30):7520–36.

1013 51. Gao E, DeAngelis GC, Burkhalter A. Parallel Input Channels to Mouse Primary Visual
1014 Cortex. J Neurosci. 2010 Apr 28;30(17):5912–26.

1015 52. Marshel JH, Garrett ME, Nauhaus I, Callaway EM. Functional Specialization of Seven
1016 Mouse Visual Cortical Areas. Neuron. 2011 Dec 22;72(6):1040–54.

1017 53. Vermaercke B, Gerich FJ, Ytebrouck E, Arckens L, Op de Beeck HP, Van den Bergh G.
1018 Functional specialization in rat occipital and temporal visual cortex. J Neurophysiol.
1019 2014 Oct 15;112(8):1963–83.

1020 54. Ghodrati M, Alwis DS, Price NSC. Orientation selectivity in rat primary visual cortex
1021 emerges earlier with low-contrast and high-luminance stimuli. Eur J Neurosci.
1022 2016;44(10):2759–73.

1023 55. Matteucci G, Zoccolan D. Unsupervised experience with temporal continuity of the
1024 visual environment is causally involved in the development of V1 complex cells. Sci
1025 Adv. 2020 May 1;6(22):eaba3742.

1026 56. DeAngelis GC, Robson JG, Ohzawa I, Freeman RD. Organization of suppression in
1027 receptive fields of neurons in cat visual cortex. J Neurophysiol. 1992 Jul 1;68(1):144–
1028 63.

1029 57. Priebe NJ, Ferster D. Mechanisms underlying cross-orientation suppression in cat visual
1030 cortex. Nat Neurosci. 2006 Apr;9(4):552–61.

1031 58. Li B, Thompson JK, Duong T, Peterson MR, Freeman RD. Origins of Cross-Orientation
1032 Suppression in the Visual Cortex. J Neurophysiol. 2006 Oct 1;96(4):1755–64.

1033 59. Busse L, Wade AR, Carandini M. Representation of Concurrent Stimuli by Population
1034 Activity in Visual Cortex. Neuron. 2009 Dec;64(6):931–42.

1035 60. Self MW, Lorteije JAM, Vangeneugden J, Beest EH van, Grigore ME, Levelt CN, et al.
1036 Orientation-Tuned Surround Suppression in Mouse Visual Cortex. J Neurosci. 2014 Jul
1037 9;34(28):9290–304.

1038 61. Samonds JM, Feese BD, Lee TS, Kuhlman SJ. Nonuniform surround suppression of
1039 visual responses in mouse V1. J Neurophysiol. 2017 Dec 1;118(6):3282–92.

1040 62. Roelfsema PR, Holtmaat A. Control of synaptic plasticity in deep cortical networks. Nat
1041 Rev Neurosci. 2018 Mar;19(3):166–80.

1042 63. Matsui T, Ohki K. Target dependence of orientation and direction selectivity of
1043 corticocortical projection neurons in the mouse V1. Front Neural Circuits [Internet].
1044 2013 [cited 2018 Jan 26];7. Available from:
1045 https://www.frontiersin.org/articles/10.3389/fncir.2013.00143/full

1046 64. Glickfeld LL, Andermann ML, Bonin V, Reid RC. Cortico-cortical projections in mouse
1047 visual cortex are functionally target specific. Nat Neurosci. 2013 Feb;16(2):219–26.

1048 65. Ji W, Gămănuţ R, Bista P, D'Souza RD, Wang Q, Burkhalter A. Modularity in the
1049 Organization of Mouse Primary Visual Cortex. Neuron. 2015 Aug 5;87(3):632–43.

1050 66. D'Souza RD, Bista P, Meier AM, Ji W, Burkhalter A. Spatial Clustering of Inhibition in
1051 Mouse Primary Visual Cortex. Neuron. 2019 Nov 6;104(3):588-600.e5.

1052 67. Jin M, Glickfeld LL. Mouse Higher Visual Areas Provide Both Distributed and
1053 Specialized Contributions to Visually Guided Behaviors. Curr Biol. 2020 Dec
1054 7;30(23):4682-4692.e7.

1055 68. Turrigiano GG, Nelson SB. Hebb and homeostasis in neuronal plasticity. Curr Opin
1056 Neurobiol. 2000 Jun 1;10(3):358–64.

1057 69. Turrigiano GG. The Self-Tuning Neuron: Synaptic Scaling of Excitatory Synapses. Cell.
1058 2008 Oct 31;135(3):422–35.

1059 70. Hengen KB, Lambo ME, Van Hooser SD, Katz DB, Turrigiano GG. Firing Rate
1060 Homeostasis in Visual Cortex of Freely Behaving Rodents. Neuron. 2013 Oct
1061 16;80(2):335–42.

1062 71. Rasmussen R, Yonehara K. Circuit Mechanisms Governing Local vs. Global Motion
1063 Processing in Mouse Visual Cortex. Front Neural Circuits. 2017 Dec 22;11:109.

1064 72. Bar M, Biederman I. Subliminal Visual Priming. Psychol Sci. 1998 Nov 1;9(6):464–8.

1065 73. Leopold DA, O'Toole AJ, Vetter T, Blanz V. Prototype-referenced shape encoding
1066 revealed by high-level aftereffects. Nat Neurosci. 2001 Jan 1;4(1):89–94.

1067 74. Kravitz DJ, Kriegeskorte N, Baker CI. High-Level Visual Object Representations Are
1068 Constrained by Position. Cereb Cortex. 2010 Dec 1;20(12):2916–25.

1069 75. Efron B, Tibshirani R. Bootstrap Methods for Standard Errors, Confidence Intervals, and
1070 Other Measures of Statistical Accuracy. Stat Sci. 1986;1(1):54–75.

1071

1072

Supporting information captions

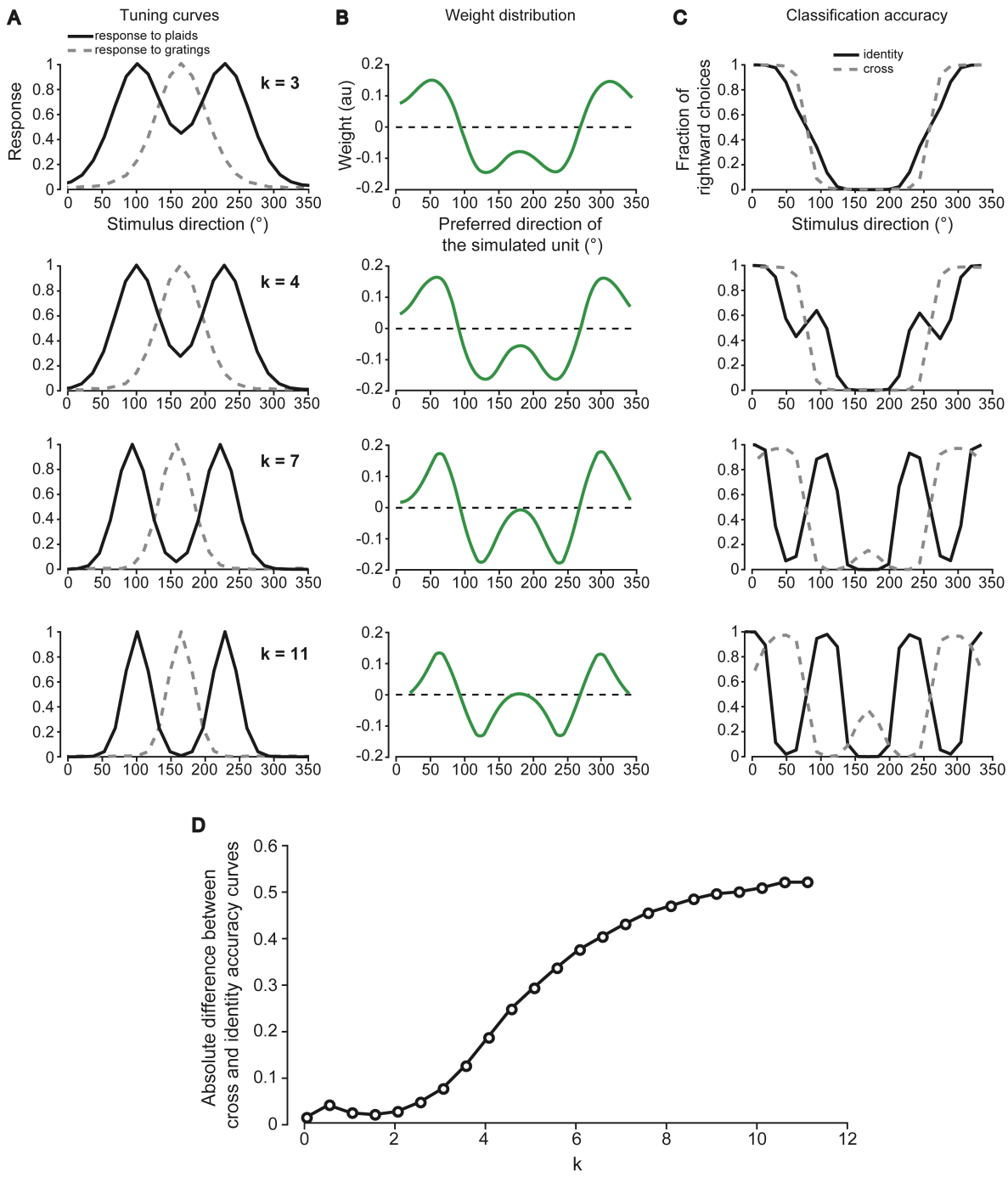

S1 Fig – Simulating the discrimination accuracy afforded by a component-based representation with different degree of direction tuning. (**A**) Example tuning curves over the direction axis, as obtained for increasingly large values of the parameter *k*, which controlled the width of the Von Mises functions used to simulate the tuning of the component cells (see main text). For each value of *k*, a population of 24 components cells was simulated, whose preferred directions

homogeneously spanned the [0º 360º] range (same as in Fig 3A). The figure shows how one of such cells (the one with preferred direction = 160º) responded to drifting gratings (gray dashed curve) and plaids (black solid curve) as a function of their direction. For *k* = 7, the curves report the same values already shown in the rows of Fig 3A (top and bottom, respectively) corresponding to the preferred direction of 160º. (**B**) Weights assigned to the 24 simulated component cells by a logistic classifier that was trained to discriminate a 0º- (rightward) from a 180º-drifting (leftward) plaid. The parameter *k* varies as indicated in A. (**C**) Fraction of times that the logistic classifier fed with the component-based representation (whose weights are shown in B) classified the test stimuli as drifting rightward (i.e., at 0º). The test stimuli were either plaids (solid black curve) or gratings (dashed gray curve) spanning the whole [0º 360º] range of directions. The parameter *k* varies as indicated in A. (**D**) Absolute difference between the pairs of curves shown in C for plaid and gratings (averaged across all tested directions) as a function of the parameter *k*.